



5th Workshop on Metallization for Crystalline Silicon Solar Cells

Fine Line Double Printing and Advanced Process Control for Cell Manufacturing

Marco Galiazzo*, Alessandro Voltan, Emiliano Bortoletto, Martina Zamuner, Marco Martire, Oscar Borsato, Matteo Bertazzo, Diego Tonini

Applied Materials Italia s.r.l., via Postuma Ovest 244, Treviso, Italy

Abstract

In this paper the latest applications of screen printing technology for solar cell metallization are reviewed. The principal achievement is 36 μm Double Printing finger width allowing +0.2% absolute efficiency gain compared to baseline Single Printing process. Dedicated rheology analysis of Ag pastes and measurements of equivalent optical finger width have been performed to have a better understanding of optimal process conditions, together with Stencil Printing experiments, showing the viability of Stencil Printing only for laboratory applications. In the last section, Advanced Printing Control is introduced as a potential enabler of controlled deposit on fingers and busbars, aiming at an increased process window and further cost savings.

© 2015 The Authors. Published by Elsevier Ltd. This is an open access article under the CC BY-NC-ND license (<http://creativecommons.org/licenses/by-nc-nd/4.0/>).

Peer-review under the responsibility of Gunnar Schubert, Guy Beaucarne and Jaap Hoornstra

Keywords: Metallization, c-Si cells, Screen Printing

1. Introduction

Although innovative approaches for solar cell metallization are constantly being introduced [1], the prominent technology to perform it in mass production is screen printing. The main reasons are cost effectiveness, extendibility to multiple cell designs, and continuous improvements in terms of consumables and equipment. The evolutionary path proposed by the ITRPV roadmap [2] starts from an emitter optimization towards higher sheet resistance values, beneficial for optimizing cell spectral properties, but leading at the same time to increased lateral resistance, which has to be compensated by adding more fingers. In order to avoid additional shading losses, these fingers should have a narrower width. At the same time, new paste generations will need an improved contact behavior to such emitters

* Corresponding author.

E-mail address: marco_galiazzo@amat.com

[3]. From a printing process standpoint it should be taken into account that reduced finger width naturally leads to yield issues such as interruptions, especially in a Single Printing (SP) configuration. For this reason Applied Materials BCS is proposing a metallization roadmap consisting of a reduced width for Double Printing (DP) fingers that are intrinsically less subject to interruptions (Fig. 1).

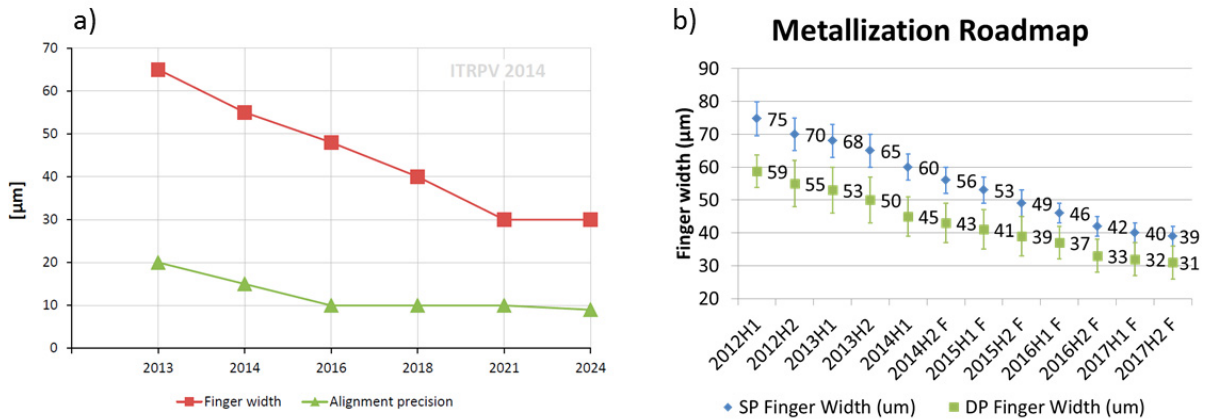


Fig. 1. (a) ITRPV roadmap for finger width reduction; (b) Applied Materials BCS roadmap for finger width reduction for SP and DP process

Based on customers data, the current finger width achieved in production in SP is around 45-55 μm, while for the DP process it is in the 40-50 μm range, with a number of fingers that is normally between 85 and 105 fingers, depending on the emitter. The reported trend for finger width reduction is of approximately 5 μm per year, and it could saturate to some extent at around 30 μm, in agreement with ITRPV prediction due to an optimization of the emitter sheet resistance value at 120 Ohm/sq.

Purpose of this work is to demonstrate viability of screen printed cells with 35 μm line width at lab scale, corresponding to the lower limit of our current performance and expected to be in mass production in approximately two years from now.

1.1 Simulation

The simulation work has been performed in order to calculate the optimum number of fingers for a certain width and aspect ratio. An electro-optical loss analysis has been carried out considering the following fixed inputs:

- Same contact and line resistivity $R_c=1 \Omega\text{cm}^2$, $R_l= 3.6 \cdot 10^{-6} \Omega\text{cm}$ for SP and DP
- Aspect Ratio, defined as the (average of maxima) finger thickness divided by average finger width, at 0.3 for SP and 0.5 for DP.
- Area Factor, defined by the ratio between the actual finger cross section and the product of finger thickness and finger width, at 0.5 for SP and 0.85 for DP
- Finger width of 45 μm for SP and 35 μm for DP, 3 busbars layout

Both for the Aspect Ratio and for the Area Factor values, the fixed inputs are based on experimental data and consistent with the results presented in section 3.1 (see Aspect Ratio data in Table 3). The number of fingers has been increased from 80 to 130 to understand if there could be a saturation of cell efficiency as it should be expected for a certain width and aspect ratio. In Fig. 2 the simulation curves have been superimposed to the red dots, representing the experimental data for SP and DP processes: by increasing the number of fingers from 95 to 105 both for SP and DP, an efficiency gain in the range of 0.05% absolute should be expected, and the efficiency delta between SP and DP should be in the range of 0.2%. On the other hand, going to 125 fingers with the same DP condition should not bring benefits as the increased shading losses would be balanced by the FF gain. In fact, a reduced finger width and increased aspect ratio would be needed in order to further increase efficiency.

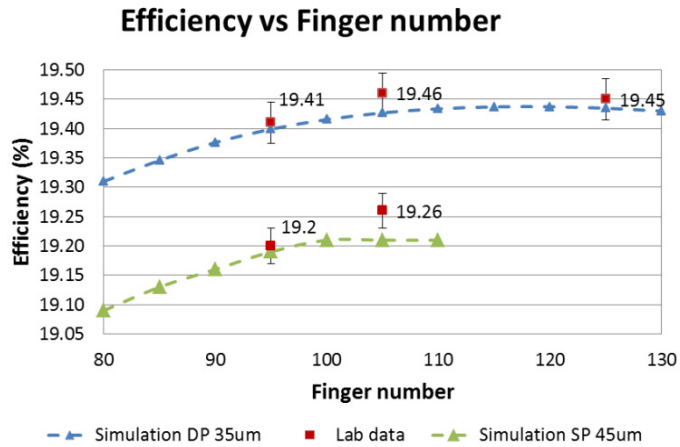


Fig. 2. Simulation data for SP (blue line) and DP (green line) cell efficiency increasing the number of fingers. Red dots represent the experimental data obtained during the tests (see section 3.1)

2. Preliminary analysis

A preliminary work has been performed in order to validate respectively: 1) the compatibility of 35 μm fingers with multiple Ag pastes of different rheology, 2) the morphological requirements needed to optimize the effective optical width of the fingers and 3) the viability of fine line printing using full open metal stencils.

2.1 Rheological analysis

The standard Ag paste (Paste A) commonly used for finger printing has been compared with a commercial paste designed for fine-line screen printing (Paste B) and a paste designed for stencil printing (Paste C).

The rheological analysis on different pastes has been carried out with plate-plate geometry, in rotational and oscillatory mode, according to [4].

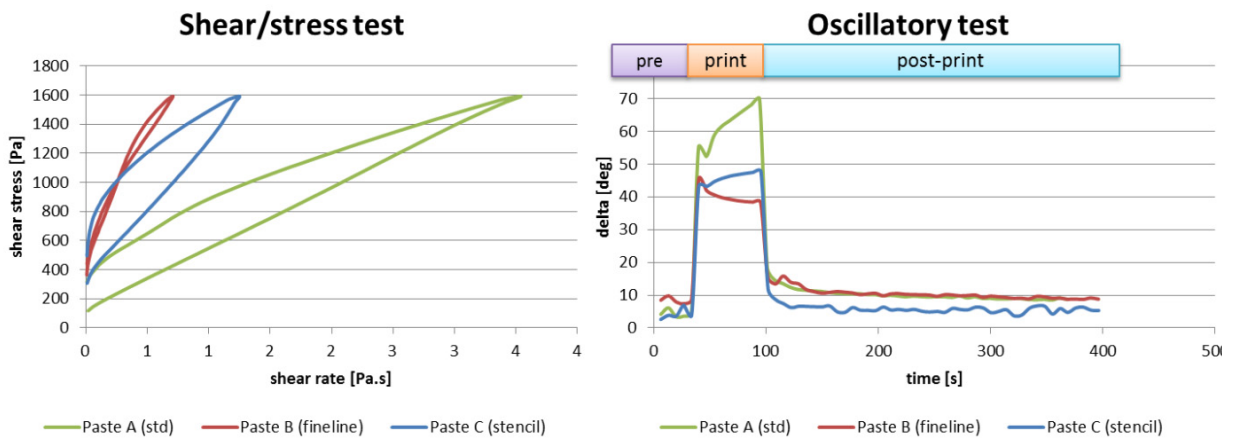


Fig. 3. (a) Shear stress vs. shear rate for different pastes – clockwise and counter clockwise shear direction reported (b) Oscillatory tests data

In Fig. 3 a) the shear stress versus shear rate test is showing a higher viscosity for paste B if compared both to paste A and C. In addition, the area comprised between the clockwise and counterclockwise rotation is giving an indication on the thixotropic behavior of the material, which is more pronounced for A and C and should translate in a different long term behavior of these pastes (i.e. more pronounced variation of viscosity over time if compared to paste B).

The oscillatory test can be divided into three phases Fig.4 b):

1. Pre-print (violet bar): it represents the period prior to the squeegee action where the paste is at rest, the frequency is 2 Hz and the amplitude is 100 μNm .
2. Print (orange bar): in this period the paste flowing through the apertures of the screen by the squeegee is simulated. The amplitude of the oscillation is increased to 20 mNm.
3. Post-print (cyan bar): is the interval where the paste recovers its structure. The amplitude is reduced to its initial value of 100 μNm

During the test the elastic and viscous behavior of the paste are measured considering the complex shear modulus ($G^* = G' + j\omega G''$). The following parameters are defined:

- G' =storage modulus [Pa] represents the elastic behavior of the paste, if it is zero the fluid is purely newtonian
- G'' =loss modulus [Pa] represents the viscous behavior of the paste and if it is zero the fluid is purely hookean
- $\Delta = \arctan G''/G'$ [deg] is the delay angle between the vector representing the applied stress and the vector representing the consequent deformation

This means that:

- If $G'' \gg G'$ then $\Delta \approx 90^\circ$ during printing: fluid behavior is more viscous
- If $G'' \leq G'$ then $\Delta \leq 45^\circ$ before and after printing: fluid behavior is more elastic

In the pre-print zone all the pastes have an elastic-like behavior, while in the printing zone the paste A is more similar to a viscous fluid if compared to both paste B and C. Interestingly, paste B is even more elastic than the paste C, and this could be counterintuitive as the former should be able to flow through narrower openings and meshes, the latter in principle should go through full open lines. In the post-print zone paste C has a better tendency to recover its initial shape and in principle this should correlate with a reduced slumping effect.

A comparative printing test at 25 μm opening width for both screen (with pastes A and B) and stencil (with paste C) has been done in order to correlate the rheological analysis with the finger morphology. Paste A printing result in Fig. 4 a) shows a significant bleeding effect at the edge of the finger and uneven height profile, while paste B in Fig. 4 b) has a good lateral confinement and uniform height profile. As expected, stencil printing with paste C has the best height uniformity due to absence of mesh (Fig. 4 c), but has more lateral widening if compared to the other pastes. This is in contrast with the findings of the previous rheological analysis, and a possible explanation will be given in section 2.3.

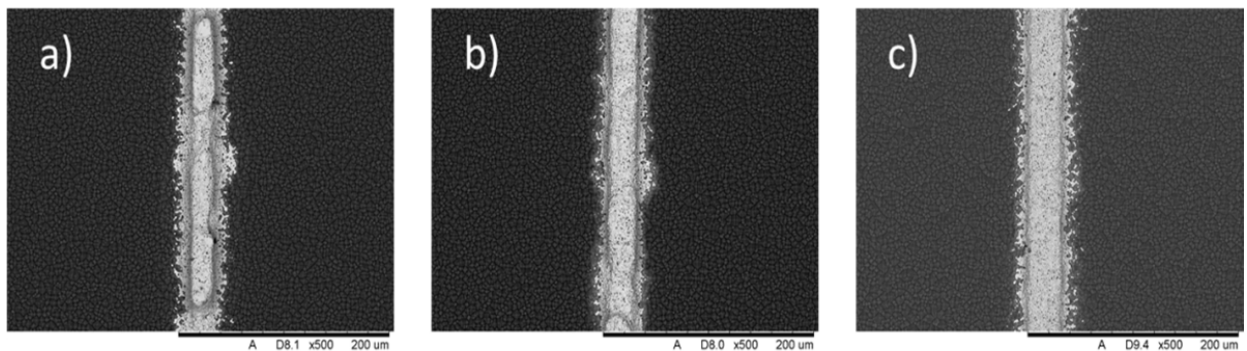


Fig. 4. SEM images of fingers printed at 25 μm opening for (a) standard Ag paste (b) fine-line printing paste and (c) stencil paste

2.2 Effective Optical Width analysis

As reported in literature [5], there is a correlation between the actual finger shape (roundness) and the finger Optical Width (OW), defined as:

$$OW = (Optical\ Factor) \times (Geometrical\ Width)$$

where the Optical Factor (OF) is a coefficient that can be experimentally determined, while the Geometrical Width is the actual finger width measured with an optical microscope. It is fundamental to consider the finger OW to take into account the secondary reflections of photons hitting the cell when it is encapsulated in the module, as represented in Fig. 5 a). In fact, a tall and round finger shape allows multiple reflections, while a flat finger does not. In conjunction with Fraunhofer ISE and Karlstad University the OW analysis has been done both for SP and DP processes with a geometrical width of respectively 65 μm and 54 μm , with standard frontside paste A. The OW analysis is based on two different approaches: μLBIC (working principle reported in Fig. 5 b) and global reflection method, as reported in [6]. From the SEM cross section pictures of Fig. 6 and the measurement results

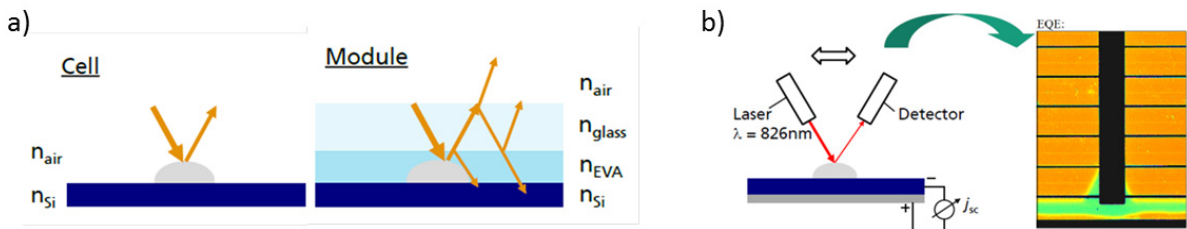


Fig. 5. (a) Photons hitting non encapsulated cells are reflected (left) and reflected back (right) when encapsulation and glass are present (b) Representation of μLBIC technique and example of External Quantum Efficiency mapping

summarized in Table 1 it is clear that due to an optimized cross section the DP process leads to a reduced OF if compared to SP. Further investigation is needed to quantify the module efficiency gain related to the reduced OW of DP.

Table 1. Experimental results on OF for SP and DP cells and mini-modules. Average of 12 measurement points per cell for GW

Lot	Paste	Geometrical Width [μm]	OF cell μLBIC	OF module μLBIC	OF cell reflection	OF module reflection
Single Printing SP	A	65	0.85	0.50	1.00	0.84
Double Printing DP	A+A	54	0.71	0.38	0.94	0.81

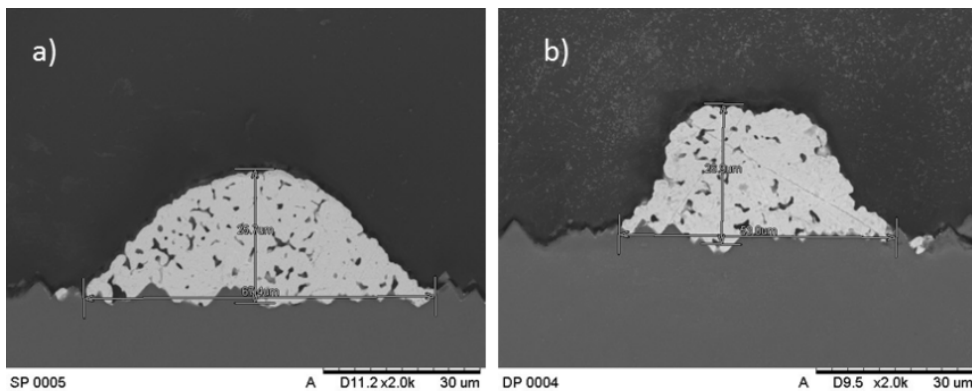


Fig. 6. SEM cross sections of: (a) 67 μm x 26 μm SP finger (b) 53 μm x 27 μm DP finger

2.3 Stencil Printing test

Due to the absence of mesh marks, the finger morphology achieved with a full open stencil has clearly the potential to enable higher efficiency and a reduction of paste consumption [7], especially when applied in a Dual Printing (DuP) configuration, where fingers and busbars are printed separately.

In this experiment we compared the performance of Screen and Stencil Printing with our reference process at 40 μm screen opening. The properties of the paste selected for the stencil process (paste C) have been already introduced in section 2.1 and basically consist of a reduced thinning behavior, suitable for printing through a full open pattern without mesh (cfr. blue lines in Fig. 3).

The morphology analysis and the electrical data are reported in Fig. 7 and Table 2 for cz-Si wafers with $90\Omega/\text{sq}$ emitter. Due to the different pastes used in the two lots, it should be noted that there could be a difference in terms of contact and line resistance. Nonetheless, the efficiency values for the stencil process are slightly higher than the reference, showing the potential benefit of this approach. The paste weight for the stencil lot is consistently higher than the Screen Printing because the high viscosity paste has been used also for the busbars, leading to unusually high busbar thickness.

Table 2. Experimental results on stencil Dual Printing compared to reference Single Printing process. Each lot data is the average of 15 wafers.

Lot	Paste	Screen	Finger	Finger	Busbar				Paste	
		Opening	Width	Thickness	Thickness	Voc	Isc	FF	Eff	Weight
		[μm]	[μm]	[μm]	[μm]	[V]	[A]	[%]	[%]	[mg]
Screen Printing	A	40	60	14	9	0.642	9.16	78.60	19.06	106
Stencil Printing	C	40	65	16	26	0.641	9.18	78.93	19.12	78+90

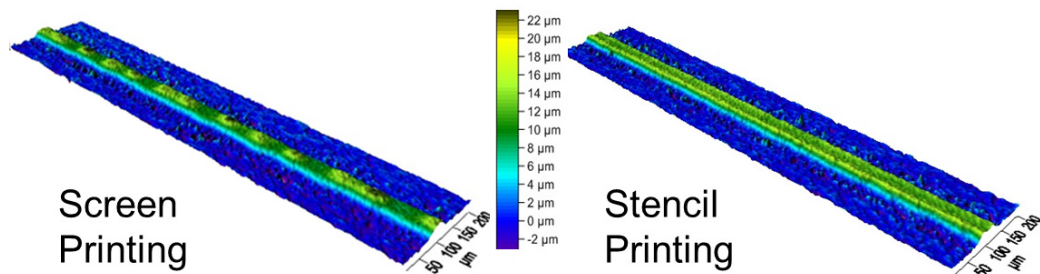


Fig. 7. 3d profilometer images of Screen and Stencil Printed finger

On the other hand, during these test we experienced several issues that prevented us from trying to extend it to narrower line widths:

- Higher line spreading for full open metal stencils – this effect is probably due to the absence of the sealing mechanism induced by the soft emulsion on the screen and leads to additional finger spreading of 5-10 μm over standard screens
- Line quality inconsistency – normally the first and the last fingers printed with the stencil have a significantly increased width due to the mechanical stress induced during the printing
- Frequent stencil cleaning – even in controlled laboratory conditions it is frequent to have paste clogging onto the stencil, probably related to particles present on the wafer surface

- Intrinsic fragility – the structure of a full open metal stencil is fragile at thicknesses $<40\ \mu\text{m}$ and due to the frequent cleaning required it is possible to break it during the tests

For these reasons, we believe stencil process is not mature yet and its applicability for mass production still needs to be proven.

3. Double Printing

After performing the preliminary assessments we identified DP as the most viable technique to achieve the initial target of $35\ \mu\text{m}$ finger width. In fact, with DP it is possible to print fine lines without interruptions even at reduced screen opening of $25\ \mu\text{m}$, virtually without Rs and FF losses. A paste formulation designed for fine line printability (paste B in Fig. 3) has been applied for SP and DP, with a slight rheology modification for versions B and B1 applied in the SP process.

In DP, paste B has been applied both for first (finger printing) and second (finger and busbars printing) layer. An alternative DP process with two different pastes has been extensively investigated [8], in order to optimize peel strength values on the busbars, but not adopted in this experiment. It should be noticed that with pastes B and B1 the SP process had a reduced opening of $35\ \mu\text{m}$, with fired finger lines that are in the range of $45\ \mu\text{m}$.

The standard process flow for 6" mono-crystalline wafers has been used: POCl diffusion with $90\ \Omega/\text{sq}$ emitter, PECVD SiN, chemical edge isolation and full Al BSF. Five different lots of 20 wafers each have been processed, with similar screen opening conditions but different number of fingers to understand the impact of this parameter in the electrical data for both SP and DP.

3.1 Morphological and Electrical results of DP

The finger morphology and electrical data are reported respectively in Fig. 8 and Table 3. The finger width of SP is slightly above $45\ \mu\text{m}$ with 0.3 Aspect Ratio, while for DP it is at around $36\ \mu\text{m}$ with 0.5 Aspect Ratio.

As expected from the simulations, the reduced finger width and increased cross section for DP leads to an efficiency gain of 0.2% absolute with respect to the DP process with the same number of fingers, when comparing for example lots SP1 and DP1 and SP2 and DP2. By increasing the number of fingers from 95 to 105 both for SP (SP1 vs SP2) and DP (DP1 vs DP2) a consistent FF improvement can be seen, leading to 0.05% absolute efficiency gain. A further increase of the number of fingers to 125, as tested in lot DP3, is not yielding additional benefit as the FF gain is negatively impacted by Isc losses, leading to the same efficiency of the previous configurations and additional paste consumption.

Table 3. Test results for Fine Line Single Printing and Double Printing processes

Lot		SP1	SP2	DP1	DP2	DP3
Process		SP	SP	DP	DP	DP
Paste		B1	B	B+B	B+B	B+B
Screen		360-16	325-16	325-16	325-16	325-16
Opening	μm	35	35	25+25	25+25	25+25
Finger number		95	105	95	105	125
Finger Width	μm	45	48	36	36	37
Finger Height	μm	14	16	18	18	20
Aspect Ratio		0.31	0.33	0.50	0.50	0.54
Busbar Height	μm	6	8	6	6	11
Peel Force	N	1.5	2.9	1.8	1.8	3.4
Jsc	mA/cm^2	38.01	37.76	38.34	38.17	37.81
Voc	V	0.644	0.642	0.643	0.643	0.643
Fill Factor	%	78.53	79.40	78.81	79.32	79.88
Efficiency	%	19.20	19.26	19.41	19.46	19.45
Paste weight	mg	100	125	99	108	149

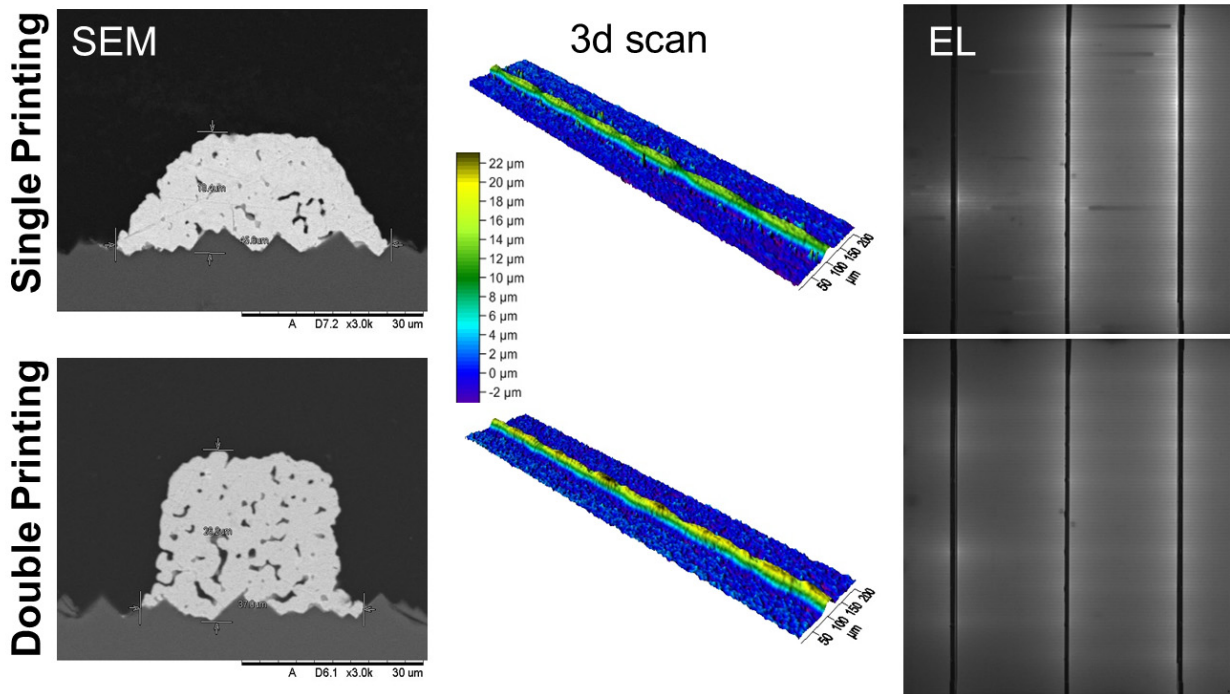


Fig. 8. Comparison between SP (top) and DP (bottom): SEM cross section, 3d laser scan and Electroluminescence

As reported in literature [9], a correlation can be seen between busbar thickness and peel force performance for each lot, with the highest values achieved for 11 μm deposit. However for all the lots, processed with 1.5 mm ribbon width, the peel force is compliant with the value specified by the standard DIN EN 50461 of 1 N per mm [10]. Measurements have been done using 180° pull angle.

A key advantage of the DP process can be seen from the Electroluminescence images in Fig. 8: there are no finger interruptions even at very narrow finger openings, increasing processing and quality yield. To our knowledge, this is one of the fundamental drivers towards adoption of DP process in production.

4. Experimental data on Advanced Printing Control

Advanced Printing Control (APC) is a patented feature based on improved software and electronics, able to control in real time the movement of the linear axes used during the printing process. As represented in Fig. 9 a), in this way it is possible to dynamically adjust the key printing parameters (pressure, speed and snap-off) during the printing stroke and increase the process flexibility. In a laboratory test APC has been applied to the SP process with standard Ag paste (paste A) in order to verify if it was possible to reduce the paste consumption without impacting significantly the cell efficiency.

The main target is to achieve finger tapering, implemented for example in [11] with ink jet printing. The basic idea is to decrease the finger cross section far from the busbars since the current density is lower in those areas. The second possibility is to decouple the finger and busbar thickness by a local variation of the printing parameters, in order to deposit the exact busbar thickness needed for a certain pull force specification. These concepts, represented in Fig. 9 b) have been evaluated by preliminary tests and simulations [12].

One interesting approach to achieve finger tapering is to simultaneously work on the thickness control, by adjusting the printing parameters with APC, and at the same time to introduce the width tapering by modifying the

screen layout, as shown in Fig. 9 c). This combination enhances the effects of APC as reported in Table 4 and Fig. 10, where the vertical tapering with the standard layout is limited to 1 μm and for the tapered layout goes to 4 μm . In all cases the APC is not impacting cell efficiency in a sensible way and will soon be tested in a manufacturing environment both for SP and DP processes.

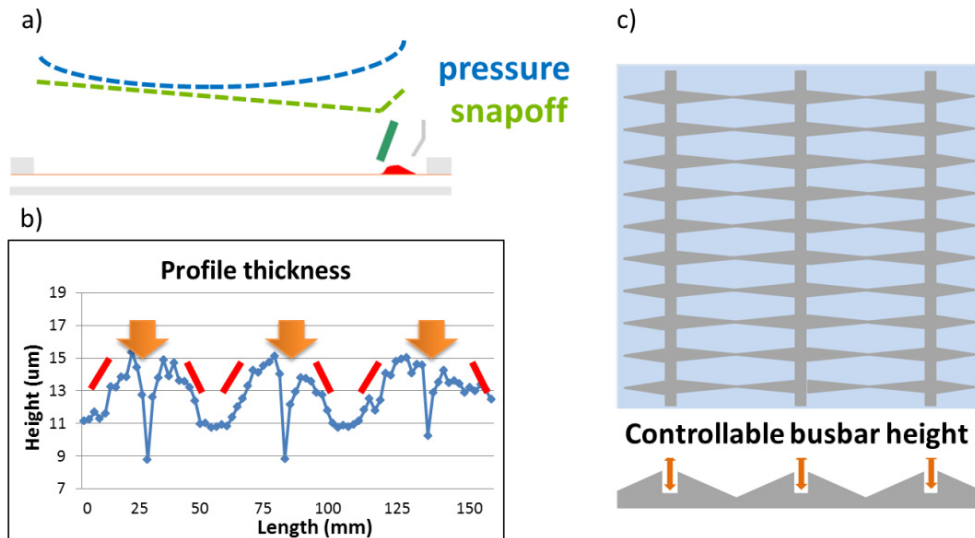


Fig. 9. (a) Schematic representation of pressure (blue) and snap-off (green) variation during printing stroke (b) thickness profile measured on the full finger length. Orange arrows represent busbar thickness, while red lines represent finger thickness variation along the profile (c) schematic of a screen layout for width tapering (top) and thickness profiling with separate control of finger and busbar thickness (bottom)

Table 4. Experimental results on APC process. Data reported are averages of 20 cells per lot.

Lot	Paste	Screen Opening [μm]	Paste Weight [mg]	Finger Width [μm]	Finger Thickness [μm]	Busbar Thickness [μm]	Voc [mV]	Isc [A]	FF [%]	Eff [%]
Standard APC off	A	40	109	63	13	8	641.4	9.17	78.84	19.05
Standard APC on	A	40	103	64-62	13-12	8	641.2	9.16	78.77	19.01
Tapered APC on	A	40+25	93	64-49	14-10	8	640.1	9.20	78.59	19.03

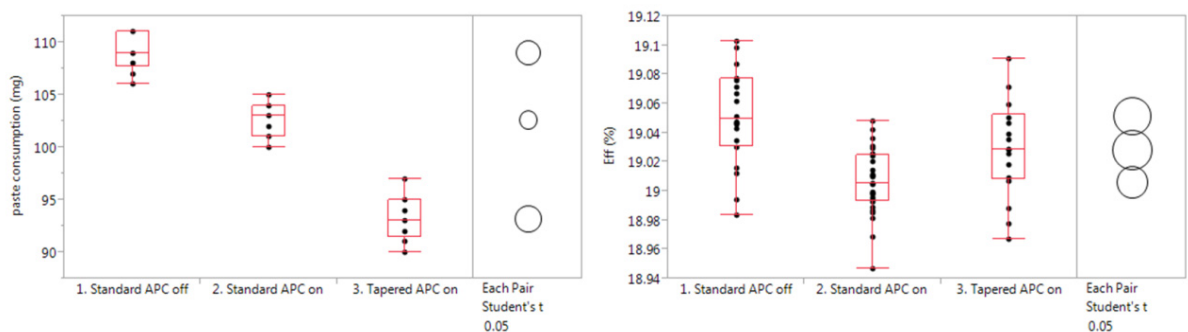


Fig. 10. Paste consumption and efficiency data for standard and APC process, with and without finger width tapering

5. Conclusions

Due to continuous efforts from paste, screen and equipment makers and the production experience of cell manufacturers, screen printing is becoming more and more sophisticated, still keeping its value and cost effectiveness.

For example, by implementing DP process finger widths in the range of 35 μ m have been achieved at lab scale, in a process that is fully compatible with mass production due to its superior quality, as shown by electroluminescence testing and cell efficiency improvement in the range of 0.2% absolute.

Evolution of screen printing is also related to the optimization of paste consumption as shown by the APC process, where a simultaneous control of finger width and thickness and busbar thickness has been achieved in SP, allowing significant paste savings for comparable cell efficiency to the standard metallization process.

Acknowledgments

The authors would like to acknowledge Heraeus for providing new generation pastes and Murakami for providing high precision screens. We would also like to thank Fraunhofer ISE and Karlstad University for the optical width analysis.

References

- [1] J. Lossen, 'Pattern Transfer Printing (PTP™) for c-Si PV Solar Cell Metallization', 5th Metallization Workshop, Konstanz (2014)
- [2] www.itrpv.net, ITRPV Edition 2014_Revision 1
- [3] M. Koenig, 'Screen Printing Ag Metallization Technology Meet the Challenges of Today's c-Si Solar Cell', 5th Metallization Workshop, Konstanz (2014)
- [4] J. Hoornstra et al., 'The Importance of Paste Rheology in Improving Fine Line, Thick Film Screen Printing of Front Side Metallization', Proc. of the 14th EUPVSEC, Barcelona (1997), pp. 832-826
- [5] A. Mette, 'Evaluation of Fine Line Printing and Plating in Pilot Production at Q-Cells', 3rd Metallization Workshop, Charleroi (2011)
- [6] R. Woehl et al., 'Analysis of the Optical Properties of Screen-Printed and Aerosol-Printed and Plated Fingers of Silicon Solar Cells, Adv. OptoElectron., vol. 2008, pp. 1-7, 2008
- [7] H. Hannebauer et al., 'Record low Ag Paste Consumption of 67.7 mg with Dual Print', Energy Procedia 43 (2013) 66 – 71
- [8] A. Voltan et al., 'Development of a Metallization Process for Super Fine Line Printing', Proc. of the 28th EUPVSEC, Paris (2013), pp. 1890-1893
- [9] P. Schmitt et al., 'Effect of Durability Testing on Solder Joint Adhesion and Failure Mode of Front Side Metallizations', Proc. of the 27th EUPVSEC, Frankfurt (2012), pp. 2058-2062
- [10] U. Eitner, L.C.Rendler, 'Peel Testing of Ribbons on Solar Cells at Different Angles: Consistent Comparison by Using Adhesive Fracture Energies', Proc. of the 29th EUPVSEC, Amsterdam (2014), pp. 3406-3408
- [11] R. Jesswein et al., 'Process Optimization of Single Step Inkjet Printed Front Contacts for Industrially Fabricated Solar Cells Leads to an Efficiency Gain of 0.3 % abs with Consumption of Less Than 60mg Silver', Proc. of the 28th EUPVSEC, Paris (2013), pp. 997-1003
- [12] M. Zamuner et al., 'Advanced Printing Control for an Optimized Cell Metallization Morphology', Proc. of the 29th EUPVSEC, Amsterdam (2014), pp. 1261-1263